Training for Planning Tumour Resection: Augmented Reality and Human Factors

Kamyar Abhari*, John S. H. Baxter, Elvis C. S. Chen, Ali R. Khan, *Member, IEEE*, Terry M. Peters, *Fellow, IEEE*, Sandrine de Ribaupierre, and Roy Eagleson

Abstract—Planning surgical interventions is a complex task, demanding a high degree of perceptual, cognitive, and sensorimotor skills to reduce intra- and post-operative complications. This process requires spatial reasoning to coordinate between the preoperatively acquired medical images and patient reference frames. In the case of neurosurgical interventions, traditional approaches to planning tend to focus on providing a means for visualizing medical images, but rarely support transformation between different spatial reference frames. Thus, surgeons often rely on their previous experience and intuition as their sole guide is to perform mental transformation. In case of junior residents, this may lead to longer operation times or increased chance of error under additional cognitive demands. In this paper, we introduce a mixed augmented-/virtual-reality system to facilitate training for planning a common neurosurgical procedure, brain tumour resection. The proposed system is designed and evaluated with human factors explicitly in mind, alleviating the difficulty of mental transformation. Our results indicate that, compared to conventional planning environments, the proposed system greatly improves the nonclinicians' performance, independent of the sensorimotor tasks performed ($p < 0.01$). Furthermore, the use of the proposed system by clinicians resulted in a significant reduction in time to perform clinically relevant tasks ($p < 0.05$). These results demonstrate the role of mixed-reality systems in assisting residents to develop necessary spatial reasoning skills needed for planning brain tumour resection, improving patient outcomes.

Index Terms—Augmented reality (AR), human factors, neurosurgical planning, neurosurgical training, tumour resection, user study, virtual reality (VR).

I. INTRODUCTION

A. Clinical Motivation

IN 2013 alone, 26 000 North Americans were diagnosed with brain cancer, resulting in 16 000 deaths [1], [2]. It is estimated that 680 000 Americans are affected by some form of primary brain or central nervous system tumours (20% of which are malignant) [3]. The five-year relative survival rate

of brain cancer is only 25–35%, making it one of the least survivable types of cancer in North America [1], [2]. Effective treatment is therefore necessary to prevent complications, which can develop with brain cancer, ranging from loss of vision and speech to paralysis and death.

Among the different courses of treatment, surgical removal of the tumour is often recommended, the resection constrained to preserve the brain's healthy tissues and functional status. Surgery is also indicated to perform a biopsy or implant a radiation source or chemotherapeutic agent [4]. Furthermore, total removal of the tumour by surgery may be the only option in the case of many benign tumours [4]. The success of these interventions greatly depends on the accuracy of planning and navigating to the target tumour. The goal of preoperative planning is to reduce intra- and post-operative complications by minimizing damage to healthy tissues and eloquent brain structures, particularly, in the case of deep-seated tumours, where planning is more critical. This is often accomplished by determining the optimal point of entry, the extent of the craniotomy, and the surgical pathways through which to advance instruments for debulking and removing the tumour.

Traditionally, in the absence of any three-dimensional (3-D) imaging to guide them, neurosurgeons learned to form a mental representation of the brain to understand the spatial relationship between the lesion and surrounding structures and landmarks. This representation is built up from their prior anatomical knowledge, while scrolling through a sequence of two-dimensional (2-D) orthogonal slices [see Fig. 1(a)], or through interaction with 3-D images of preoperative magnetic resonance or computed tomography (CT) scans presented on a computer display [see Fig. 1(c)]. The ease of use of such perceptual environments—as will be discussed in the following section—is heavily influenced by their mode of visualization and interaction. This is even more true in the case of junior residents, whose more limited experience affects their ability to quickly perform spatial reasoning. In the current standard of care, residents gradually acquire these skills over several years throughout their residency by observing expert neurosurgeons planning their approach. Meanwhile, residents rely heavily on neuronavigation systems, which may help them to decide the surgical approach, but are not designed to improve their spatial reasoning abilities.

B. Background

Interaction within an environment involves movement in some coordinate space that can be estimated relative to a *frame of reference*. To interact with the system, one must first establish a frame of reference, and, then, perform a series of *mental*
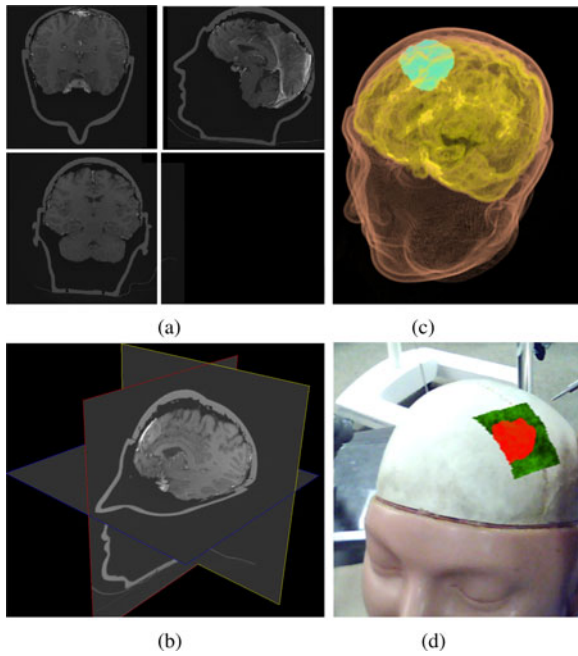
Fig. 1. Planning environments: (a) 2-D views of axial/coronal/sagittal slices, (b) XP representation of 2-D slices, (c) 3-D volume rendering, (d) overlay of virtual images on the real video in an AR environment.

transformations. These transformations correspond to mentally rotating, translating, or scaling an entity to transform its spatial location and orientation from one frame of reference to another. Performing these transformations requires mental resources that may cause *cognitive overload* and reduce performance if the capacity of the working memory is exceeded [5]. In the realm of neurosurgery, the choice of display (and its underlying methods of *visualization* and *interaction*) is perhaps one of the most important, yet underappreciated, factors in task performance. This is of particular importance in neurosurgical planning, in which the entire process can vary significantly, depending on the modes of visualization and interaction. Conventionally, planning is performed by scrolling through 2-D orthogonal slices (2-D), or interacting with 2-D crossed planes (XP) or 3-D volume or surface rendered images (3-D) [6] [see Fig. 1(a)–(c)]. In this paper, in addition to these conventional approaches, we explore the possibility of using a mixture of *virtual-reality* (VR) and *augmented-reality* (AR) environments in surgical planning of tumour resection interventions, with a particular focus on AR. Unlike VR, where the entire scene is computationally generated, AR is often described as an environment, in which the view of the real world is enhanced by *overlaying* computer-generated information. One such approach is purposed to complement the available information with computer generated images, providing a rich view of the operative field, and so facilitating the performance of a surgical task. An example of an AR environment is illustrated in Fig. 1(d). AR is sometimes referred as *mixed reality*, a concept described and popularized by Milgram and Kishino [7]. In their proposed reality-virtuality continuum, the mixed-reality spans from environments, in which the virtual

information augments the real view (AR) to those where real information augments the virtual scene [augmented-virtuality or (AV)].

C. Related Work

Since the introduction of immersive environments in 1957 [8], a body of work has been devoted to the development of VR and AR environments for surgical training, planning, and navigation (refer to [9]–[13] for more comprehensive reviews). In the realm of neurosurgery, a number of AR simulators have been developed to allow surgeons to plan and rehearse a surgical approach prior to the actual operation, with the *VR-workbench* [14], *Dextroscope* [15], and *ImmersiveTouch* [16] platforms being a few examples. In these simulators, the user must wear a pair of active stereo glasses, while holding a set of controllers positioned beneath a half-silvered mirror. By doing so, it is then possible to visualize and manipulate patient volumetric images simultaneously, where the visual and haptic environments are registered. Although these systems provide a safe training and planning environment, user interaction is limited due to restricted working space, small field of view, and sometimes absence of head tracking. A more natural method of interaction was proposed by Hinckley *et al.* [17], which involved holding a miniature size head mannequin in one hand, and a plastic plate in the other hand to virtually slice open the volumetric representation of patient data presented on a computer display. Although more intuitive, the interaction appeared unnatural, whenever the operator's perspective and the virtual slice were misaligned. To reduce the risk associated with the insertion of surgical tools, Shamir *et al.* have proposed an AR planning environment described in [18] and [19].

AR also has been shown to facilitate the intraoperative navigation in minimally-invasive neurosurgery. In [20], for instance, preoperative images of brain landmarks and critical structures were superimposed on a live video stream of the patient's head (or the surgical site in [21]), and displayed on a screen during surgery. The *microscope-assisted guided interventions* system [22] is another example, where 3-D preoperative images were overlaid into both eyepieces of the binocular optics of a surgical microscope. Shahidi *et al.* [23] made use of AR to improve the endoscopic view by registering real endoscopic and virtual preoperative images together. Bichlmeier *et al.* [24] proposed a so-called *virtual mirror* to display a desired perspective in endoscopic procedures when the virtual object cannot be viewed due to physical restrictions, a concept similar to the use of mouth mirrors in dentistry. In the *reality augmentation for surgical procedure* system [25], a tracked head-mounted display (HMD) was employed to display the neuroanatomical structures on a head phantom. In this system, a camera and an LED infrared flash is incorporated into the HMD, preventing the lag between rendering virtual and real images, as well as the line of sight issue of the optical trackers. Lerotic *et al.* made use of a novel nonphotorealistic technique for visualizing virtual object, while maintaining salient anatomical details of the exposed surface [26]. Paul *et al.* [27] augmented intraoperative views of the operative

field over preoperative images, and projected the result onto a computer display. This compensated for the limited field of view, providing context to the intraoperative images.

D. Hypothesis and Objective

1) Hypothesis: We hypothesize that, compared to conventional planning environments, the proposed AR system offers a more intuitive visualization and interaction approach, resulting in improved task performance to optimize surgical planning of tumour resection interventions.

2) Objective: In this paper, we propose an AR system to assist novice surgeons in developing the cognitive skills demonstrated by experts in planning tumour resection interventions. Experiments are conducted to evaluate the proposed system by measuring the user performance, in both AR and conventional environments.

II. MATERIALS AND METHODS

In this section, a general framework for understanding the interaction and visualization aspects of planning environments in brain tumour resection is presented. This framework is used to guide the design, implementation, and evaluation of the AR environment described subsequently.

A. Action and Perception in Planning Environments

Different aspects of interactive systems, specifically interaction and visualization, can support different levels of visuospatial actions and perception. *Action* involves interacting with the system to update the visualization, which requires mental transformation from the self to the display frame of reference (e.g., moving the mouse to the right in order to rotate the image). *Perception*, on the other hand, involves observing the effects of the interaction and reconciling them, performing mental transformation to match the visualization with the desired 3-D representation of the image, or validating that information estimated from one viewpoint is legitimate in another. The continual cycle of interaction with the system to perform a task is extremely flexible and adaptive, and aspects of action and perception are present in each of the underlying mental processes associated with interactive systems [28].

B. Mental Processes in Planning Environments

Using an interactive system often involves executing a collection of mental processes. The hypothetical model shown in Fig. 2 represents three primary underlying mental processes in determining the optimal point of entry and surgical path within a given planning environment. *Perceptual integration* involves assembling a 3-D mental representation of the patient's brain by continuously obtaining and processing views. This representation is necessary for *action planning*, that is, mentally formulating and identifying the optimal surgical path and point of entry. The specific goals to be addressed are based on a number of criteria described in Section II-F, and may involve continuous mental processing of the information within a 3-D space. Additionally, one must *coordinate between reference frames* to
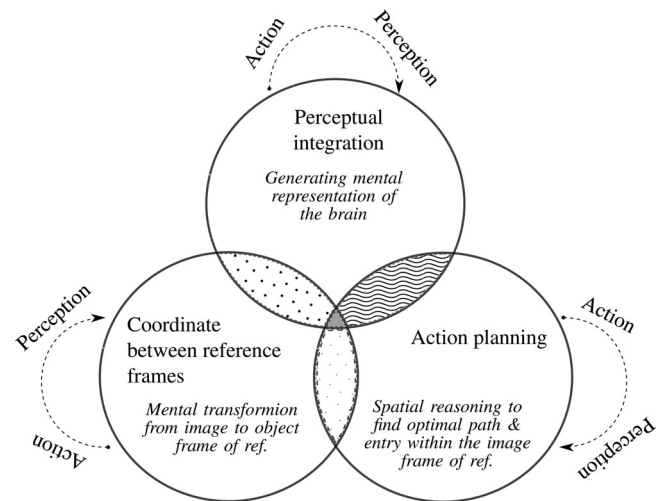

Fig. 2.   Underlying mental processes in planning environment.

transform the mental representation of the optimal path/point of entry from the display frame of reference to the object frame of reference, i.e., the patient's skull in the operation room. These processes may occur simultaneously or sequentially depending on the preferences and experience of the user. Nevertheless, minimizing the mental demand elicited by these processes is necessary to design an intuitive planning system.

C. Mental Demands in Planning Environments

Perceptual integration in 2-D involves generating a 3-D mental representation of the brain by scrolling through 2-D images, while recalling previous views. This process imposes a high demand on working memory and can be facilitated by positioning and interacting with these 2-D images within a 3-D context (e.g., the XP environment). Visualizing the brain in 3-D with the help of volume rendering can further lower the demand on spatial reasoning, reducing the need for perceptual integration (e.g., the AR and 3-D environments) .

The *coordination of reference frames* required for transforming the formulated optimal path and point of entry into the physical frame of reference (e.g., patient's head or a head phantom) is almost negligible in the AR environment. This is because preoperative images are often overlaid directly on the physical object, eliminating the transformation between the two. In contrast, extensive mental work is needed in the case of 2-D, XP, and 3-D environments, particularly for novice operators, as they must transform the view from the display into the physical frame of reference.

Furthermore, exploring data via interaction with the phantom in AR environments mimics direct hand manipulation. Such a natural everyday human behavior can further reduce the mental demand of relevant judgment tasks in *action planning*. It also provides extraretinal signals of different sources (such as proprioceptive information), enhancing the perception of depth when paired with certain visualization techniques (details are discussed in the next section). Although a more realistic representation of the brain in 3-D facilitates the process of action
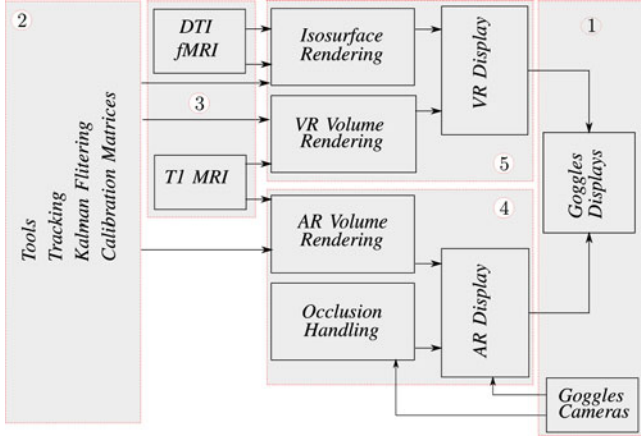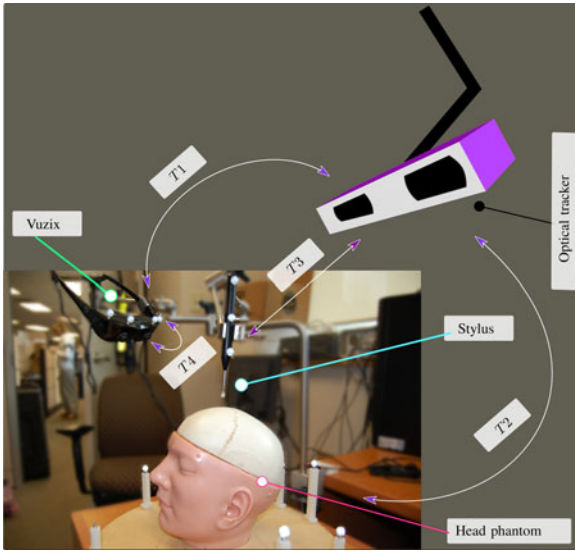
Fig. 3. Implementation diagram.

Fig. 4. AR system consists of a pair of AR goggles, a head phantom, a stylus, and an optical tracker. The transformation matrices of $T1$, $T2$, and $T3$ are given using the optical tracker, while $T4$ is computed using camera calibration.

planning compared to 2-D and XP, less intuitive modes of interaction in these conventional environments demand a high degree of mental effort to formulate the surgical approach.

D. System Implementation

Our AR system comprises several modules and components as shown in Figs. 3 and 4. These modules can be broken down into five overarching categories:

1) The AR goggles and other tools,
2) Tracking and calibration components,
3) Medical image components,
4) AR visualization modules, and
5) VR visualization modules.

The AR goggles (Vuzix 920AR, Vuzix corporation, Rochester, NY, USA) consist of a set of stereoscopic cameras (480×640) that provide a video feed into the planning system. In addition, the Vuzix goggles contain stereoscopic displays (600×800) on the opposite side on which the system's renderings can be displayed. Other tools include a head phantom and a stylus, giving the user physical analogs for virtual representations of the patient and aperture, respectively. Additionally, a set of foot pedals was incorporated to allow the user to interact with the system, while maintaining their viewpoint of the phantom. Tracking input to this system includes physical coordinates from an optical tracking system (Polaris, Northern Digital Inc., Waterloo, Canada), which relate to the AR glasses, tracked stylus, and head phantom through preacquired calibration matrices. The calibration process for the AR glasses is described in [29]. The tracked transform was smoothed using a Kalman filter framework to reduce jitter. The state vector is the pose information, encoded using a 4×1 quaternion for rotation and 3×1 for translation. The process model is the identity matrix, and the measurement model is the actual measurement from the optical tracking system. This tracking information is used to manage a virtual coordinate system, in which the AR goggles and the head phantom dictate the position of the renderer viewpoint and the position of the medical image data, respectively.

The system is capable of rendering T_1 weighted MRI images, using volume rendering integrated with a 2-D transfer function [30], and displaying associated fMRI activation clusters and white matter tracts. T_1 weighted acquisitions are clinically used for detecting brain tumours and planning brain tumour resection.

In VR mode, there are two separate renderers. First, the isosurface renderer converts a polyhedral representation of the DTI tracts, eloquent fMRI regions, and the stylus to a 2-D rendering of these objects. The depth buffer (z-buffer) for this rendering is then passed to the VR volume renderer, which uses ray casting, and 2-D transfer functions to render the tumour and skin in the T_1 weighted MRI. This rendering style supports opacity values and, thus, renders the background as transparent and the skin translucent, allowing internal structures to be visualized. These renderings are then merged together, overlaying the volume rendering on the isosurface rendering. The result is a 3-D rendering of the phantom with a layer of translucent skin through which the tumour, white matter tracts, and eloquent cortical regions can be seen. A virtual representation of the stylus is incorporated that corresponds to its location relative to the head phantom.

In AR mode, the volume rendering acts similarly, but is sensitive to a virtual aperture at the stylus tip. The same ray casting technique is used, but rays can terminate prematurely if they do not pass through the aperture. This conveys the appearance of a *window* into the head phantom at the tip of the stylus, which is sensitive to the position and orientation of the Vuzix glasses relative to the phantom. The occlusion handling system is designed to identify regions of the video feeds that are occluded by the participant's hands (see Fig. 6[1]). This is accomplished via hue-based thresholding, which masks out the blue surgical gloves worn by the participant (refer to Section II-E2 for more details). The final step in the AR display is to merge the AR volume rendering with the occlusion sensitive video achieved by masking out occluded areas in the AR volume rendering, marking

---

[1]In this paper, the stereoscopic views are illustrated in left-right-left fashion, corresponding to left-right-left AR cameras and displays.
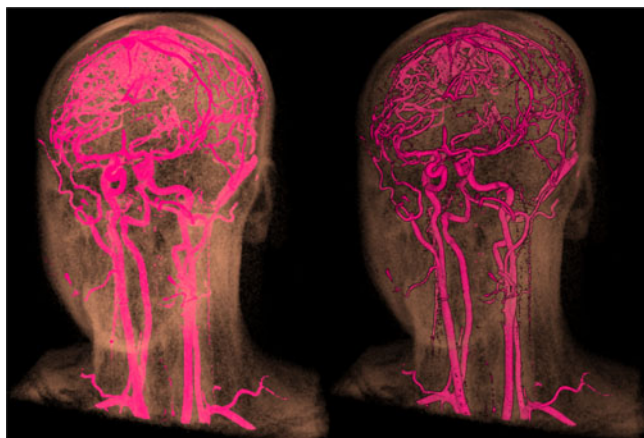
Fig. 5. Example of contour enhancement using cel shading in volumetric images (*left*: before enhancement, *right*: after enhancement).

Fig. 6. Example of hue-based occlusion handling.

Fig. 7. Example of use of a keyhole with grid lines to promote the sensation of depth.

them as transparent. Subsequently, the AR volume rendering is overlaid on the AR video feed to the goggles. Furthermore, as part of our visualization approach, users have an option to substitute the virtual window with a set of grid lines (see Fig. 7) to improve the perception of depth (refer to Section II-E for more details).

The desired rendering system is selected by the user; a foot pedal can be used to toggle between the AR and VR display modes. This foot pedal also can be used to lock the position of the stylus, allowing for the aperture to remain locked in position, giving the user the opportunity to use both hands to manipulate the head phantom. The tracking status is provided at the bottom of the visualization, indicating when a tracked object has valid line-of-sight with the tracker (green), has lost tracking information (red), or has its position locked (blue).

E. Perceptual Cues and Considerations in AR

While effective visualizations can dramatically improve the outcome and efficiency of interactive environments, poor visualization approaches may result in cognitive overload or misinterpretation [31]. This is even more profound in AR environments, as subtle conflicts between real and virtual images result in incorrect depth perception, degrading performance [11]. Although many studies have discussed the issue of depth perception in AR systems [32], [33], problems still persist [11]. In HMD-based AR systems, for instance, *accommodation-vergence conflict* may cause depth distortion, hindering performance [34]. Accommodation is an involuntary movement of the eye to keep objects in focus by changing the shape of the lens. Vergence is the inward/outward movement of both eyes in order to fixate on a single point. Normally, these two eye movements act in synchrony, providing coherent cues for the perception of depth. In HMD-based systems, however, the observer's eyes accommodate to the screens, while constantly diverging and converging to maintain the binocular vision on a single object, providing incoherent depth cues. This has been shown to be a major drawback of HMD-based AR systems [32]. Such conflicts, however, can be mitigated if more dominant visual cues convey the desired
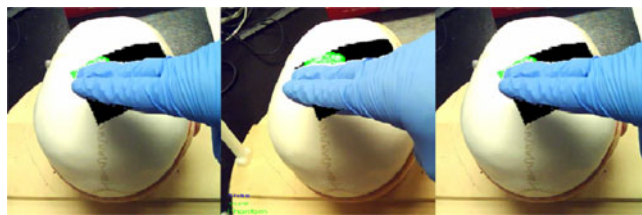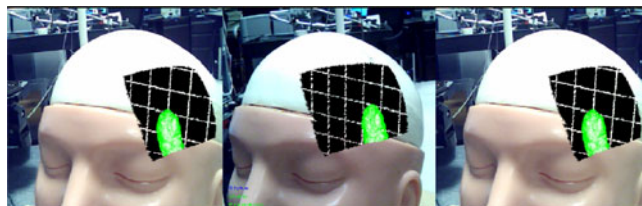
sense of depth. This section is therefore devoted to describe the visualization techniques used in the AR system to improve the perception through the most effective depth cues [35] including *stereopsis*, *motion parallax*, and *occlusion*.

1) Cel Shading: In our previous studies [36], [37], we showed that contour enhancement can facilitate the perception of relative depth. This is even more profound in HMD-based ARs as the effect of contour enhancement is accentuated when paired with stereopsis [37]. Thus, in this paper, a nonphotorealistic technique called cel shading [37] is employed to enhance the contours of the target tumour (see Fig. 5).

2) Occlusion Handling: Partial blockage of one object's view by another object or *occlusion* is the strongest cue in perceiving the relative proximity of objects [35]. One well-known problem with the use of AR environments for medical applications is the occlusion of operators' hands or medical devices by virtual images, resulting in depth misperception. To resolve this issue, hue-based thresholding was employed to detect and mask the blue surgical gloves worn by the participant (see Fig. 6). This *occlusion handling* technique was inspired by the work described in [38].

3) Grid Lines: The apparent displacement of objects against their background, or *motion parallax*, is an effective and unambiguous cue, providing rich information about relative depth. In our AR environment, motion parallax occurs both when user makes lateral head movement with respect to the phantom (subject motion), and when the phantom translates relative to the user (object motion). Studies have shown that the former type of motion provides stronger sense of depth [39], [40], perhaps due to the fact that interaction with the phantom provides nonvisual information, such as proprioceptive, enhancing the perception in concert with motion parallax [41], [42]. Regardless of source of motion, a stronger sense of parallax can be evoked if the apparent displacement of the tumour is accentuated relative to its background. To this aim, a set of grid lines was placed behind the target tumour, amplifying the motional difference between the tumour and its background (see Figs. 7 and 8).
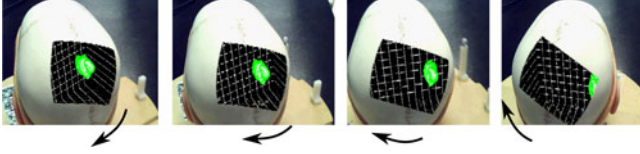
Fig. 8. Visualizing grid lines behind the tumour evokes a strong sense of motion parallax, while interacting with the phantom.
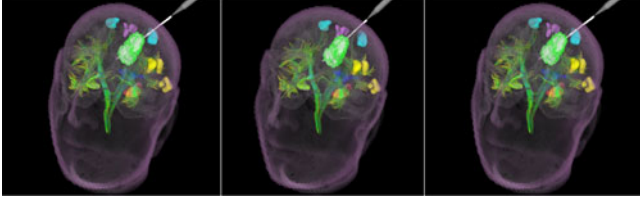

Fig. 9. Example of the VR mode to visualize DTI tracts, functional areas, and virtual stylus.

4) Keyhole: Williams [43] has shown that performing tasks that demand a high degree of visual attention lowers the accuracy of peripheral vision from 75% to 36%, shrinking the field of view. Therefore, when a visuospatial task requires focused attention (i.e., high cognitive consumption), it is undesirable to present a large amount of data in the periphery. This issue is addressed in the literature by presenting information through a virtual window [44]–[46]. Similarly, in the proposed AR system, virtual images were placed inside the phantom to present the inner view within a *keyhole* (see Fig. 7).

5) Virtual Reality: In AR environments, new information is superimposed on the real scene. This can extend the information to the user, but can also add clutter to an already complicated view, causing *information overload* [47]. Additionally, clutter in 3-D can lead to visual occlusion of the target, degrading perceptual performance [48]. Accordingly, the amount of information presented in our proposed AR system was restricted to the target tumour and the keyhole. To visualize additional information, however, a VR display was employed, in which the real world-view is removed by turning OFF the video feed and halting the early ray termination process. In the VR mode, the user can visualize DTI tracts, functional areas of the brain, and the stylus' trajectory with no clutter (see Fig. 9). Users may benefit from both the AR and VR by toggling between these two modes of visualization.

F. Evaluation Studies

Linte *et al.* [13] identified the lack of clinical evaluation and the difficulty of 3-D information visualization and manipulation as two major barriers in introducing AR technology into clinical environments. Conducting user studies is therefore necessary to validate the benefit of AR environments compared to other approaches, and to provide insight toward perceptually-correct visualization methods [13].

As discussed previously, the process of planning usually requires spatial reasoning in order to interact with preoperative images, and transform the mental representation of the chosen path and entry point into the patient and operation environment. While 2-D displays are currently considered the de facto standard for visualization and interaction with preoperative data, AR environments are believed to provide a more intuitive alternative. Although many research groups have proposed different AR environments for medical interventions (see Section I-C), evaluation studies are necessary to understand the system's shortcomings and facilitate the translation into clinical practice. This motivated us to assess the effectiveness and efficiency of the AR system against conventional planning environments[2], exploring their underlying mental load (preliminary results have been presented in [49] and [50]).

Our experiments involve three different phases. In phases 1 and 2, nonclinicians interacted with synthetic images, whereas phase 3 involved clinicians and nonclinicians performing clinically-relevant tasks by examining patient-specific data. These experiments were designed to address three major planning criteria:

1) determining the shortest possible distance to the target tumour,
2) aligning the surgical tool with the longest axis (LA) of the tumour, and
3) specifying a trajectory that would avoid critical functional areas and white matter DTI tracts.

These criteria are the main considerations in planning tumour resection to minimize damage to healthy brain tissues.

1) Phase 1 *and* 2*: Data:* Stimuli consisted of the CT images of the head phantom with synthetic structures analogous to patient anatomical data (e.g., an ellipsoid representing the target tumour). The use of CT images with synthetically created anatomical structures allowed for more control over the experimental design.
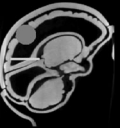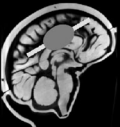
Methodology: Each experiment involved 12 trials per subject (3[tasks] × 4[environments]) through which participants (8 male/2 female, no prior training) were presented with a randomized collection of synthetic phantom images. Each trial isolated one criterion by defining the task as either determining the *LA* of the tumour or the *shortest distance* (SD) from the skull to the tumour or the maximal distance from the tumour to a critical structure and so avoiding it. The ground truth for the LA, SD, and avoidance (AV) tasks were determined, respectively, by computing the primary eigenvector of the tumour using principle component analysis, segmenting the skull and computing its distance to the tumour, and finding the maximum Hausdorff distance between the tumour and the critical structure (see Table I). Subjects were asked, first, to investigate the data to estimate the optimal point of entry and surgical path and, then, place and orient the stylus on the head phantom, disclosing their chosen location and orientation.

The rationale behind the second phase was to examine whether AR environments can facilitate the planning process, even if one makes use of a computer to assist with the estimation of the optimal point of entry and surgical path. Therefore, unlike phase 1, the ground truth, whether the SD, LA, or maximal

---

[2]Neither occlusion handling nor grid lines were incorporated into the AR system for these evaluation studies.

TABLE I

Middle Row: CT Images of the Phantom With a Synthetic Ellipsoid (LA), a Sphere (SD), or a Sphere and a Tube (AV) Were Generated to be Used as Stimuli in Phase 1; *Bottom Row*: the True LA of the Ellipsoid, SD From the Sphere to the Skull, and Maximal Hausdorff Distance From the Sphere to the Tube (AV) Were Shown in Phase 2 (Images are Only a few Examples From the 2-D Environment)

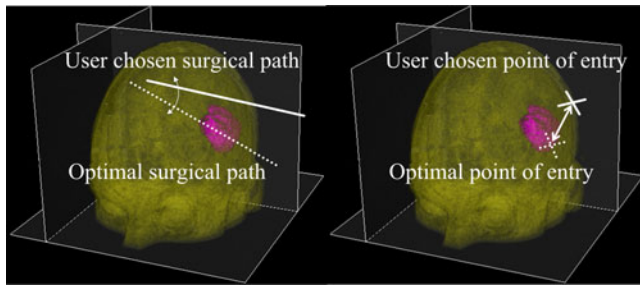| Task	LA (*finding the longest axis of target*)	SD (*finding the shortest distance from target to skull*)	AV (*finding the max. Hausdorff distance between target & adjacent tube*)
e.g. in 2D, phase 1			
e.g. in 2D, phase 2			

Fig. 10. Rotational (*left*) and translational error (*right*) were used as metrics to measure users' performance.
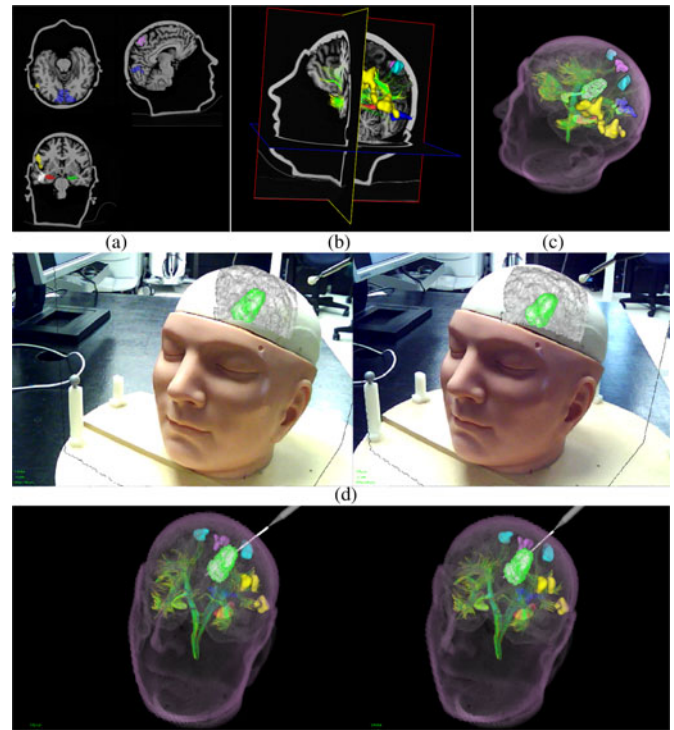

Fig. 11. Visualization of patient-specific data in (a) 2-D, (b) XP, (c) 3-D, and (d) AR (left and right images correspond to left and right views of the AR cameras/displays) environments in phase 3.

distance, was illustrated via synthetic lines (see Table I). Such visual assistance eliminated the need to formulate the optimal path and entry point, reducing the cognitive load mainly to the mental transformation from a display frame of reference (the computer's screen or HMD's display) to the object frame of reference (head phantom).

In both phases, the stimuli, the planning environment, and the task were randomized and counterbalanced to minimize the effects of learning and fatigue.

Analysis: As illustrated in Fig. 10, user performance was measured based on the *translational error*, that is the Euclidean distance between the optimal points of entry and those selected by users (in millimeter), and the *rotational error*, that is, the deviation between the optimal surgical path and the angle selected by participants (in degrees).

2) Phase 3: Data: Our medical image input comes from the medical image computing and computer intervention (MICCAI) DTI challenge workshop[3] to generate a total of 112 different patient-specific cases by resizing and relocating the segmented tumour samples. All images were processed *a priori* to segment the tumour, relevant eloquent areas, and white matter tracts.

This process was performed by an expert to create clinically relevant scenarios, and also to control the proximity of the tumour to surrounding eloquent areas. Such regions include functional areas of visual cortex, hippocampi, and areas representing language and the peripheral limbs, as well as the tractography of corticospinal, uncinate fasciculus, arcuate fasciculus, and the Meyer's loop (see Fig. 11). Including DTI tracts and pseud-ofMRI data gives context to the experiments, increasing the ecological validity. For the purposes of this study, the MRI images were registered and visualized within a CT scan of a head phantom.

Methodology: Each experiment involved 64 trials per subject[4] (2[tasks] $\times$ 4[environments] $\times$ 8[repeated trials]), in which 21 participants were asked to either identify the LA of the tumour and align the stylus with their chosen axis or determine the SD to the tumour and place the stylus on their chosen location over the head phantom. The pool of subjects included seven clinicians (three neurosurgeons with >five years of practice, three residents and one fellow with >two years of training) and 14 novice graduate students (i.e., nonclinicians).

Analysis: Rotational error for LA and translational error for SD were measured after excluding inaccessible points of entry, such as face, ears, and neck. In addition to accuracy metrics, the response time (RT) was also recorded, indicating the overall time one took to explore the images, formulate the optimal points of entry or surgical paths, and transform the results to the phantom frame of reference.

---

[3]MICCAI 2010–2011, permission is granted.

[4]Forty eight trials for one of the clinicians.

Index of Performance: Because our task has a complicated 3-D structure, we redefined different aspects of Fitts' Law [51]. First, we express the index of difficulty as

$$ID = H[P(x)] - H[P(x|x \in A)] \qquad (1)$$

where $H[\cdot]$ is the entropy functional, $P(x)$ is the uniform distribution over possible stylus tips/trajectories, and $P(x|x \in A)$ is the uniform distribution over possible stylus tips/trajectories that meet the criterion for success. Moreover, our methodology was an extension of Fitts' classical *click in the box* task [51]. Subjects were asked to specify their position and angles as quickly and accurately as possible, but there was no prespecified region that would correspond to a hit or miss within a region. Instead, the *effective width* of their targeting was derived from the mean of their position and angular responses. We thereby define a pseudocriterion for each participant, specifically that $x \in A$ if and only if the error associated with x is less than or equal to the participant's average error. Accordingly, we can define the index of performance for each user as

$$I_P = \frac{1}{T}ID = \frac{1}{T}\left(H[P(x)] - H[P(x|x \in A)]\right). \qquad (2)$$

For the rotational error used in aligning the surgical trajectory with the LA, the index of performance can be determined analytically from the average angular error, μ (refer to the appendix for more details)

$$I_P = \frac{1}{T}\log_2\left(\frac{1}{1 - \cos(\mu)}\right). \qquad (3)$$

For translation, the value of $H[P(x)] - H[P(x|x \in A)]$ is determined via a Monte Carlo simulation similar to that employed to determine the gold standard entry point (refer to the appendix for more details).

III. RESULTS AND DISCUSSIONS

A. Phase 1

The overall performance was calculated by computing the rotational and translational error (see Fig. 12). Since our hypothesis, i.e., the AR system lowers *both* rotational and translational error, may be interpreted methodologically as two independent hypotheses, the Šidàk correction was applied to control the type I error. Let the significance threshold for each test be $p = 0.01$; then, a stricter *p*-value based on Šidàk correction would be: $\beta = 1 - \sqrt{1 - 0.01} \approx 0.005$, leading to a combined level of significance of 1%.

A two-way multivariate ANOVA indicated that the environment had a significant effect on accuracy (rotational/translational error: $p < 0.005$). Post hoc analysis using Tukey HSD test revealed that users performed significantly more accurately in AR and 3-D environments, indicating their lower rate of mental processes compared to XP or 2-D environments. Furthermore, no interaction was observed ($p > 0.05$) between the task and the environment. Furthermore, no significant difference was observed between the visualization environments in terms of the task completion time [overall time (s)]: 178.8 ± 131.1 [2-D],
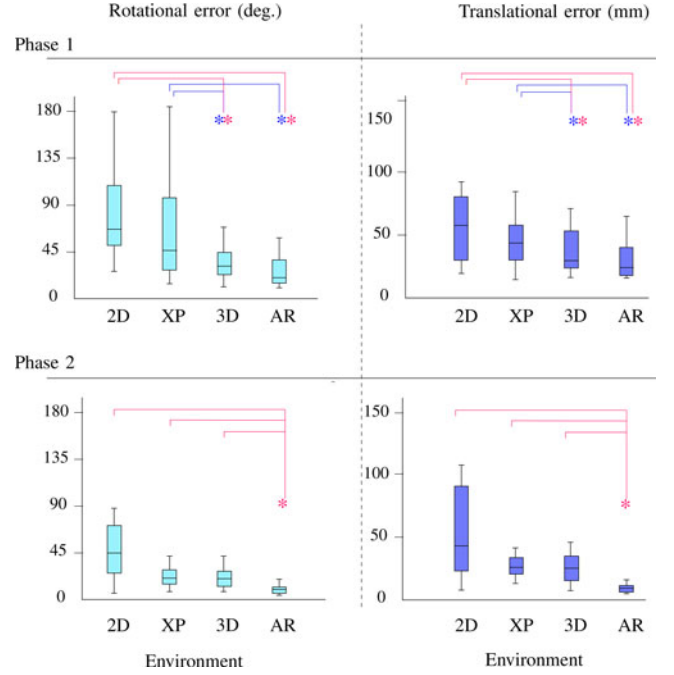
Fig. 12. Overall rotational and translational errors observed in phase 1 (top) and phase 2 (bottom).

204.1 ± 172.7 [XP], 143.6 ± 106.8 [3-D], 170.1 ± 104.6 [AR]).

B. Phase 2

In phase 2, the task was restricted to a response that was dependent on *coordinating between different reference frames* to transform images from the display to the physical context. In this phase, AR was significantly superior to the other planning environments, reducing user dependent error. Both translational and rotational errors were significantly lower in AR compared to other environments ($p < 0.005$, see Fig. 12). Unlike phase 1, interaction analysis revealed that the level of performance within the 2-D and XP environments depended in part upon the task performed. Moreover, no significant difference was observed between the visualization environments in terms of the task completion time [overall time (s)]: 111.5 ± 83.8 [2-D], 123.6 ± 74.8 [XP], 78.7 ± 46.6 [3-D], 77.2 ± 52.7 [AR]).

C. Phase 3

Phase 3 involved clinicians and nonclinicians performing clinically-relevant tasks by examining patient-specific data. The result of this phase is depicted in Fig. 13. A two-way multivariate ANOVA indicated that RT was significantly affected by both *expertise* and *environment* ($p < 0.005$). The choice of *environment* also significantly affected the rotational error, as well as I_p for both tasks ($p < 0.05$). Regardless of expertise, the mean accuracy was higher in AR compared to other environments (see Table II), however, no significant difference was observed between these environments, perhaps due to insufficient power as a result of small sample size, or because of longer experimentation
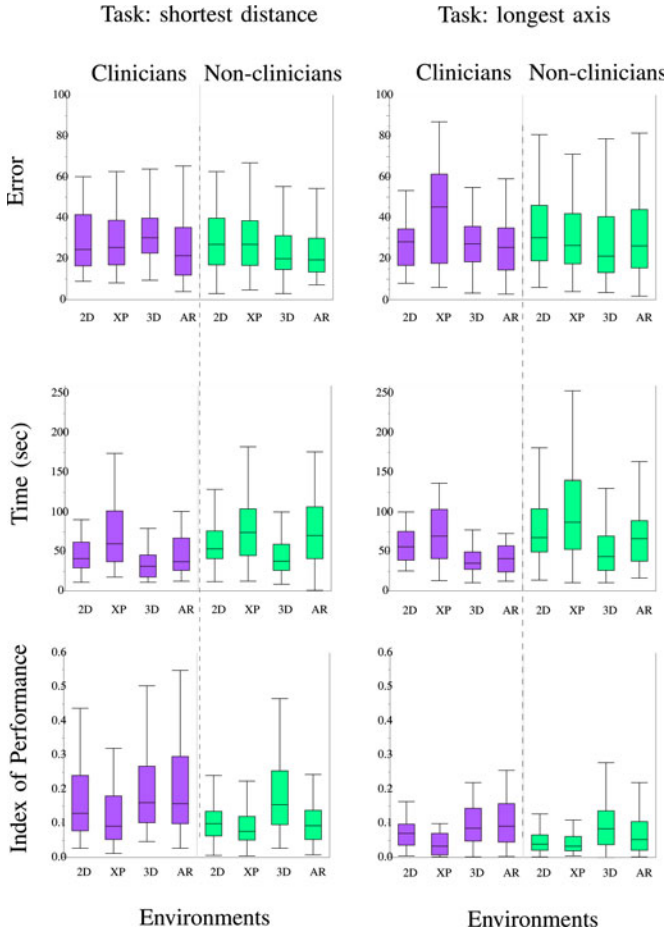
Fig. 13. *Top*: Translational (*left*) and rotational error (*right*); *Middle*: Time for SD (*left*) and LA (*right*); *Bottom*: I_p for SD (*left*) and LA (*right*).

TABLE II
AVERAGE ROTATIONAL AND TRANSLATIONAL ERROR (PHASE 3)

Rotational error (^{o}), $\mu \pm \sigma$			
AR	3-D	2-D	XP
38.07 ± 24.22	41.19 ± 23.74	42.80 ± 23.25	44.98 ± 23.74
Translational error (mm), $\mu \pm \sigma$			
AR	3-D	2-D	XP
37.29 ± 31.48	38.94 ± 27.73	39.48 ± 26.98	40.63 ± 32.91

time, which when coupled with poor ergonomics of the AR goggles resulted in fatigue and higher rate of error.

Unlike SD experiments, significant interaction was observed in LA ($p < 0.05$), indicating that users' performance in selecting the LA within different environments depended in part on their level of expertise. Post hoc analysis using Tukey HSD test revealed that, regardless of the task performed, clinicians performed significantly faster and better (i.e., higher I_p) than nonclinicians within the AR and 2-D environments ($p < 0.05$). This improvement of I_p within the 2-D environment was not surprising given the fact that clinicians are highly accustomed to interpreting 2-D images. Furthermore, regardless of the task performed, clinicians performed significantly faster within the AR and 3-D environments compared to the XP, whereas

nonclinicians performed significantly faster within the 3-D environment compared to the XP and 2-D ($p < 0.05$). In addition, for the restricted range of eccentricities displayed, no correlation was observed between the eccentricity of the tumours and performance in any of the environments.

The translational and rotational errors reported in this study appear to be relatively high for IGI applications. However, this is due to the nature of the metrics defined. For instance, one can imagine that selecting an entry point that corresponds to the second S to the target could be very distant from the optimal point of entry, resulting in a large translational error. To this aim, we defined two other metrics as the followings. A translational error as the difference (in *milliliter*) between the length of the optimal path and the path chosen by the user, and a rotational error as the difference (in *milliliter*) between the section of the optimal and chosen path cutting through the tumour. Analyzing data based on these two metrics led to very similar results, illustrating the robustness of our initial metrics.

Overall, following observations can be made based on the results.

1) *Phase* 1: The improvement of performance in 3-D and AR indicates that appropriate visualization methods (i.e., AR, 3-D) can significantly facilitate the perception and mental transformation of the target location and orientation and its spatial relationship with surrounding anatomical context;

2) *Phase* 2: The improvement of performance in AR demonstrates that AR can significantly facilitate the process of perceptual integration and coordination between frames. In other words, AR is superior to the other planning environments in assisting nonclinicians to generate a mental representation of the brain, and transform it from a display to the patient frame of reference. In addition, observing an interaction between the task and the environment in 2-D and XP indicates their lack of generic usability. In contrast, this suggests the use of AR for applications that involve tasks with multiple and possibly conflicting criteria;

3) *Phase* 3: The improvement of speed in AR and 3-D compared to the XP and 2-D regardless of expertise, and the task performed illustrates the potential impact of such environments in increasing the efficiency of planning. One unexpected result, however, was the relationship between the 2-D and XP. Our conceptual models predicted that XP would have improved performance compared to 2-D afforded by presenting information in a 3-D context. Although the action mechanisms in XP were more expressive, they were also more complex, leading to lengthened RT across all participant groups. This could be mitigated in practice as users become more familiar with this mode of interactive viewing.

IV. CONCLUSION

In this paper, we designed, developed, and evaluated an AR environment, by which novice physicians can practice and improve their basic spatial skills, increasing their cognitive ability to perform neurosurgical planning. Design of the proposed environment was accomplished by careful consideration of the

cognitive and perceptual capacities and limitations of human observers. To evaluate our system, a number of experiments were conducted, in which subjects performed relevant spatial judgment tasks using the proposed system along with conventional approaches. Our results indicate that AR environments could facilitate the task of planning brain tumour resections according to clinically-relevant criteria. Nonintuitive environments, on the other hand, were shown to be inefficient and less effective. The proposed work is a preliminary step toward the clinical use of AR environments, particularly, in facilitating brain tumour resections.

APPENDIX
DERIVATION OF I_p

I_p for LA task-based on the rotational error and RT Let A be space of acceptable x

$$P(x \in A) = \oint \frac{1}{2\pi} \mathrm{d}x$$
$$= \int_0^\mu \int_0^{2\pi} \frac{1}{2\pi} \sin(\theta) \mathrm{d}\phi \mathrm{d}\theta$$
$$= \int_0^\mu \frac{2\pi \sin(\theta)}{2\pi} \mathrm{d}\theta$$
$$= \int_0^\mu \sin(\theta) \, \mathrm{d}\theta$$
$$= 1 - \cos(\mu)$$

which implies

$$ID = H[P(x)] - H[P(x|x \in A)]$$
$$= -\int P(x) \log(P(x)) \, \mathrm{d}x$$
$$+ \int_A \frac{P(x)}{P(x \in A)} \log\left(\frac{P(x)}{P(x \in A)}\right) \mathrm{d}x$$
$$= -\int P(x) \log(P(x)) \, \mathrm{d}x +$$
$$\frac{1}{P(x \in A)} \int_A P(x) \log(P(x)) \, \mathrm{d}x - \log(P(x \in A))$$
$$= -\int_0^\pi \int_0^{2\pi} \frac{1}{2\pi} \log\left(\frac{1}{2\pi}\right) \sin(\theta) \, \mathrm{d}\theta \, \mathrm{d}\phi +$$
$$\frac{1}{1 - \cos(\mu)} \int_0^\mu \int_0^{2\pi} \frac{1}{2\pi} \log\left(\frac{1}{2\pi}\right) \sin(\theta)$$
$$\mathrm{d}\theta \, \mathrm{d}\phi - \log(1 - \cos(\mu))$$
$$= \log(2\pi) - \log(2\pi) - \log(1 - \cos(\mu))$$
$$= \log\left(\frac{1}{1 - \cos(\mu)}\right)$$
$$I_p = \frac{1}{\mathrm{RT}} ID = \frac{1}{\mathrm{RT}} \log\left(\frac{1}{1 - \cos(\mu)}\right).$$

I_p for SD task using the translational error and RT Let $|X|$ = Total number of points uniformly sampled over the skull, $|A|$ = number of points sampled within the region with a radius of average translational error

$$ID = H[P(x)] - H[P(x|x \in A)]$$
$$= -\int P(x) \log(P(x)) \, \mathrm{d}x$$
$$+ \int_A \frac{P(x)}{P(x \in A)} \log\left(\frac{P(x)}{P(x \in A)}\right) \mathrm{d}x$$
$$\approx -\sum_{x \in X} \frac{1}{|X|} \log\left(\frac{1}{|X|}\right) + \sum_{x \in A} \frac{1}{|A|} \log\left(\frac{1}{|A|}\right)$$
$$= \log\left(\frac{|X|}{|A|}\right)$$
$$= \log\left(\frac{|A| + |\neg A|}{|A|}\right)$$
$$I_p = \frac{1}{\mathrm{RT}} ID = \frac{1}{\mathrm{RT}} \log\left(1 + \frac{|\neg A|}{|A|}\right).$$

ACKNOWLEDGMENT

REFERENCES

[1] Canadian cancer statistics. (2013). Canadian Cancer Society, Public Health Agency of Canada. [Online]. Available: http://goo.gl/hkiWep
[2] Cancer facts and figures 2013. (2013). American Cancer Society. [Online]. Available: http://goo.gl/z3vHVc
[3] Primary brain and central nervous system tumors diagnosed in the united states in 2004–2008. (2012). Central Brain Tumor Registry of the United States. [Online]. Available: http://goo.gl/mM3Pgd
[4] A. Quinones-Hinojosa, *Schmidek and Sweet: Operative Neurosurgical Techniques: Indications, Methods and Results (Expert Consult—Online and Print)*. Philadelphia, PA, USA: Elsevier Health Sciences, 2012. [Online]. Available: http://books.google.ca/books?id=4sKQSY-zdvgC
[5] D. Reisberg, *The Oxford Handbook of Cognitive Psychology*. London, U.K: Oxford Univ. Press, 2013.
[6] T. M. Peters, "Image-guidance for surgical procedures," *Phys. Med. Biol.*, vol. 51, no. 14, pp. R505–R540, 2006.
[7] P. Milgram and F. Kishino, "A taxonomy of mixed reality visual displays," *IEICE Trans. Inf. Syst.*, vol. 77, no. 12, pp. 1321–1329, 1994.
[8] H. L. Layer, "Sensorama simulator," U.S. Patent 3 050 870, Aug. 28, 1962. [Online]. Available: https://www.google.com/patents/US3050870
[9] J. H. Shuhaiber, "Augmented reality in surgery," *Arch. Surg.*, vol. 139, no. 2, pp. 170–174, 2004.
[10] R. T. Azuma *et al.*, "A survey of augmented reality," *Presence*, vol. 6, no. 4, pp. 355–385, 1997.
[11] T. Sielhorst *et al.*, "Advanced medical displays: A literature review of augmented reality," *Disp. Technol. J.*, vol. 4, no. 4, pp. 451–467, 2008.
[12] M. Kersten-Oertel *et al.*, "DVV: A taxonomy for mixed reality visualization in image guided surgery," *IEEE Trans. Vis. Comput. Graph.*, vol. 18, no. 2, pp. 332–352, Feb. 2012.
[13] C. A. Linte *et al.*, "On mixed reality environments for minimally invasive therapy guidance: Systems architecture, successes and challenges in their implementation from laboratory to clinic," *Comput. Med. Imag. Graph.*, vol. 37, no. 2, pp. 83–97, 2013.
[14] T. Poston and L. Serra, "The virtual workbench: Dextrous VR," in *Proc. Conf. Virtual Reality Softw. Technol.*, 1994, pp. 111–121.

[15] A. T. Stadie *et al.*, "Virtual reality system for planning minimally invasive neurosurgery," *Neurosurgery*, vol. 108, pp. 382–394, 2008.

[16] C. Luciano *et al.*, "Design of the immersivetouch: A high-performance haptic augmented virtual reality system," presented at the *11th Int. Conf. Human-Comput. Interact.*, Las Vegas, NV, USA, 2005.

[17] K. Hinckley *et al.*, "The props-based interface for neurosurgical visualization," *Stud. Health Technol. Informat.*, vol. 39, pp. 552–562, 1997.

[18] R. R. Shamir *et al.*, "Reduced risk trajectory planning in image-guided keyhole neurosurgery," *Med. Phys.*, vol. 39, no. 5, pp. 2885–2895, 2012.

[19] R. R. Shamir *et al.*, "Trajectory planning with augmented reality for improved risk assessment in image-guided keyhole neurosurgery," in *Proc. IEEE Int. Symp. Biomed. Imag., Nano Macro*, 2011, pp. 1873–1876.

[20] W. Grimson *et al.*, "Image-guided surgery," *Sci. Amer.*, vol. 280, no. 6, pp. 54–61, 1999.

[21] R. A. Kockro *et al.*, "Dex-ray: Augmented reality neurosurgical navigation with a handheld video probe," *Neurosurgery*, vol. 65, no. 4, pp. 795–808, 2009.

[22] P. J. Edwards *et al.*, "Design and evaluation of a system for microscope-assisted guided interventions (MAGI)," *IEEE Trans. Med. Imag.*, vol. 19, no. 11, pp. 1082–1093, Nov. 2000.

[23] R. Shahidi *et al.*, "Implementation, calibration and accuracy testing of an image-enhanced endoscopy system," *IEEE Trans. Med. Imag.*, vol. 21, no. 12, pp. 1524–1535, Dec. 2002.

[24] C. Bichlmeier *et al.*, "The virtual mirror: A new interaction paradigm for augmented reality environments," *IEEE Trans. Med. Imag.*, vol. 28, no. 9, pp. 1498–1510, Sep. 2009.

[25] C. R. Maurer, Jr., *et al.*, "Augmented-reality visualization of brain structures with stereo and kinetic depth cues: System description and initial evaluation with head phantom," *Med. Imag. Int. Soc. Opt. Photon.*, vol. 445, pp. 445–456, 2001.

[26] M. Leroticet al., "Pq-space based non-photorealistic rendering for augmented reality," in *Proc. Med. Image Comput. Comput.-Assisted Intervention Conf.*, 2007, pp. 102–109.

[27] P. Paul, "Augmented virtuality based on stereoscopic reconstruction in multimodal image-guided neurosurgery: Methods and performance evaluation," *IEEE Trans. Med. Imag.*, vol. 24, no. 11, pp. 1500–1511, Nov. 2005.

[28] R. Eagleson, "Perceptual capacitites and constraints in augmented reality biomedical displays," presented at the *Innovations Patient Care, Eng. Phys. Sci. Med. Aust. Biomed. Eng. Conf.*, Christchurch, New Zealand, 2008.

[29] E. C. Chen, "An augmented reality platform for planning of minimally invasive cardiac surgeries," *Proc. SPIE, Med. Imag., Int. Soc. Opt. Photon.*, vol. 8316, pp. 831617–831617, 2012.

[30] J. S. Baxter *et al.*, "A unified framework for voxel classification and triangulation," *Proc. SPIE, Med. Imag., Int. Soc. Opt. Photon.*, vol. 7964, pp. 796436–796436, 2011.

[31] C. Ware, *Information Visualization: Perception for Design*. New York, NY, USA: Elsevier, 2012.

[32] E. Kruijff *et al.*, "Perceptual issues in augmented reality revisited," in *Proc. IEEE 9th Int. Symp. Mixed Augmented Reality*, 2010, vol. 9, pp. 3–12.

[33] D. Drascic and P. Milgram, "Perceptual issues in augmented reality," *Proc. Electron. Imag, Sci. Technol., Int. Soc. Opt. Photon.*, vol. 2653, pp. 123–134, 1996.

[34] M. Mon-Williams and J. R. Tresilian, "Ordinal depth information from accommodation?" *Ergonomics*, vol. 43, no. 3, pp. 391–404, 2000.

[35] S. Nagata, "How to reinforce perception of depth in single two-dimensional pictures," *Proc. Soc. Inf. Disp.*, vol. 25, no. 3, pp. 239–246, 1984.

[36] K. Abhari *et al.*, "Perceptual enhancement of arteriovenous malformation in MRI angiography displays," *Proc. SPIE, Med. Imag., Int. Soc. Opt. Photon.*, vol. 8318, pp. 831809–831809, 2012.

[37] K. Abhari *et al.*, "Visual enhancement of MR angiography images to facilitate planning of arteriovenous malformation interventions," *ACM Trans. Appl. Percept.*, submitted for publication, 2014

[38] O. Kutter *et al.*, "Real-time volume rendering for high quality visualization in augmented reality," presented at the *Int. Workshop Augmented Environ. Med. Imag., Augmented Reality Comput.-Aided Surg.*, New York, NY, USA, 2008.

[39] B. Rogers *et al.*, "Motion parallax as an independent cue for depth perception," *Perception*, vol. 8, no. 2, pp. 125–134, 1979.

[40] H. Ono and M. J. Steinbach, "Monocular stereopsis with and without head movement," *Percept. Psychophys.*, vol. 48, no. 2, pp. 179–187, 1990.

[41] V. Cornilleau-Peres and J. Droulez, "The visual perception of three-dimensional shape from self-motion and object-motion," *Vis. Res.*, vol. 34, no. 18, pp. 2331–2336, 1994.

[42] M. R. Mine *et al.*, "Moving objects in space: Exploiting proprioception in virtual-environment interaction," in *Proc. 24th Annu. Conf. Comput. Graph. Interacti. Techn.*, 1997, pp. 19–26.

[43] L. J. Williams, "Tunnel vision induced by a foveal load manipulation," *Human Factors, J. Human Factors Ergonom. Soc.*, vol. 27, no. 2, pp. 221–227, 1985.

[44] M. Bajura *et al.*, "Merging virtual objects with the real world: Seeing ultrasound imagery within the patient," *ACM SIGGRAPH Comput. Graph.*, vol. 26, no. 2, pp. 203–210, 1992.

[45] C. Bichlmeier *et al.*, "Contextual anatomic mimesis hybrid in-situ visualization method for improving multi-sensory depth perception in medical augmented reality," in *Proc. IEEE 6th Int. Symp. Mixed Augmented Reality*, 2007, pp. 129–138.

[46] L. T. De Paolis *et al.*, "Augmented visualization of the patient's organs through a slidingwindow," presented at the *Workshop Vis. Model. Vis.*, Braunschweig, Germany, 2009.

[47] S. Mann and S. M. Nnlf, "Mediated reality," 1994.

[48] R. Rosenholtz *et al.*, "Measuring visual clutter," *J. Vis.*, vol. 7, no. 2, p. 17, 2007.

[49] K. Abhari *et al.*, "Use of a mixed-reality system to improve the planning of brain tumour resections: Preliminary results," in *Augmented Environments for Computer-Assisted Interventions*, New York, NY, USA: Springer, 2013, pp. 55–66.

[50] K. Abhari *et al.*, "The role of augmented reality in training the planning of brain tumor resection," in *Augmented Reality Environments for Medical Imaging and Computer-Assisted Interventions*, New York, NY, USA: Springer, 2013, pp. 241–248.

[51] P. M. Fitts, "The information capacity of the human motor system in controlling the amplitude of movement." *J. Exp. Psychol.*, vol. 47, no. 6, pp. 381–391, 1954.

Kamyar Abhari received the Master's of Science degree in biomedical engineering from the University of Manitoba, Winnipeg, MB, Canada, in 2008. He is currently working toward the Ph.D. degree at Western University, London, ON, Canada. He is a Member of the Robarts Research Institute, London. His primary research interests include surgical visualization and human–computer interaction in image-guided surgeries.

John S. H. Baxter received the Bachelor's degree in software engineering from the University of Waterloo, Waterloo, ON, Canada, in 2012. He is currently working toward the Ph.D. degree at the Biomedical Engineering Graduate Program, Western University, London, ON, Canada. He is a Member of the Robarts Research Institute, London. His current research interests include biomedical-image processing, statistical-image representation, and image segmentation.

Elvis C. S. Chen received the Ph.D. degree in computer science from Queens University, Kingston, ON, Canada, in 2007.

He works in the field of image-guided interventions, by applying techniques in robotics and computer graphics to the field of surgery. His research interests include joint kinematics, ultrasound-guided needle interventions, tool calibration and tracking, and vision-guided laparoscopy. He is currently a Research Associate at the Robarts Research Institute, London, ON, with cross appointment with Western University, London.

Ali R. Khan (M'14) received the Ph.D. degree in engineering science from Simon Fraser University, Burnaby, BC, Canada, in 2011.

His research is focused on the development of intelligent image processing and analysis technologies, and their application in the diagnosis and treatment of neurological disorders. His research interests include computational anatomy, quantitative magnetic resonance imaging, diffusion tensor tractography, and image registration. He is currently an Assistant Professor at the Department of Medical Biophysics, Western University, London, ON, Canada, and is affiliated with the Robarts Research Institute, London. He is an Associate Member of the IEEE Engineering in Medicine and Biology Society Technical Committee on Biomedical Imaging and Image Processing.

Sandrine de Ribaupierre received the MD degree from the University of Geneva, Geneva, Switzerland.

After a Neurosurgery residency in Lausanne, Switzerland, she completed an epilepsy fellowship from the Fondation Rothschild, Paris, France, then a pediatric neurosurgery fellowship from the Hospital for Sick Children, Toronto, Canada. She is c]urrently an Assistant Professor at the Division of Neurosurgery, University of Western Ontario, London, ON, Canada, working as a Pediatric Neurosurgeon with some involvement in pediatric and adult trauma and adult epilepsy surgery. Her main research interests include virtual reality as an educational tool, such as to teach neuroanatomy to medical students, as well as surgical simulation for residents. She is collaborating with CSTAR, Robarts, and the Centre for Brain and Mind.

Terry M. Peters (S'72–M'73–SM'97–F'09–LF'14) is currently a Scientist at the Imaging Research Laboratories, Robarts Research Institute, London, ON, Canada, and a Professor at the Departments of Medical Imaging, Medical Biophysics, and Biomedical Engineering, Western University, ON. From the past 30 years, he has been working in the field of image-guided surgery and therapy within the Robarts Imaging Research Laboratories. His lab has expanded more than the past 13 years to encompass image-guided procedures of the heart, brain, and abdomen.

Roy Eagleson received the Ph.D. degree supervised by Zenon Pylyshyn from the University of Western Ontario, Centre for Cognitive Science, London, ON, Canada, in 1992. In 2014, he was an Associate Professor with the Faculty of Engineering, Western University, London, doing his research with the Robarts Research Institute, London, a Scientist and a Principal Investigator at Canadian Surgical Technologies and Advanced Robotics Research Center, London Health Sciences Centre, Lawson Health Research Institute, London, and Collaborator with the UWO Brain and Mind Institute. His research interest includes 3-D biomedical visualization and surgical simulation, human–computer interface design for telerobotics and telesurgery, haptic interfaces, and programmable graphical interfaces (GPU programming).